Super

FINAL REPORT
TO
UTAH DEPARTMENT OF NATURAL RESOURCES
SALT LAKE CITY, UTAH

STUDIES OF WINTERTIME STORMS OVER THE TUSHAR MOUNTAINS OF UTAH

MARCH 1986

DAVID C. ROGERS
ROBERT M. RAUBER
LEWIS O. GRANT

DEPARTMENT OF ATMOSPHERIC SCIENCE
COLORADO STATE UNIVERSITY
FORT COLLINS, COLORADO

FINAL REPORT

TO

UTAH DEPARTMENT OF NATURAL RESOURCES

SALT LAKE CITY, UTAH

STUDIES OF WINTERTIME STORMS OVER THE TUSHAR MOUNTAINS OF UTAH

David C. Rogers

Robert M. Rauber

Lewis O. Grant

Department of Atmospheric Science

Colorado State University

Fort Collins, Colorado

March 6, 1986

EXECUTIVE SUMMARY

Colorado State University has been involved in the Utah/NOAA program as a research partner in the last two field seasons. This report presents the results of two research tasks that addressed data from the 1985 field season. The tasks were to (1) estimate the maximum possible amount of precipitation that could have been obtained through optimum weather modification techniques over the entire season, and (2) assemble a case study description of one STORM event.

The results of this research are as follows. For task (1), the supercooled liquid water flux over the Tushar Mountains was estimated from three-hour averages of the radiometer and rawinsonde observations. With optimum cloud seeding, we hypothesized that all of this water would have been converted to precipitation. The amount of liquid water represented by this flux over the two-month project was 17,000 acre feet, or about 45 percent of the total annual runoff in the Beaver River watershed. Of the 35 three-hour samples during the 1985 season, 50 percent of the liquid water flux was contained in the largest 5 samples. Thus, in order for the operational program to be effective, it must be capable of responding to essentially all seeding opportunities; it would be a major loss if the few large cases were missed. Most of the liquid water corresonded with 700 mb temperatures warmer than about -7°C. In the absence of stratification, the liquid water flux was uncorrelated with precipitation rate.

For task (2), STORM 9 was described as a large scale, deep cold frontal storm, not a simpler orograhic cloud system. Four phases of the

but see P. 14

STORM were differentiated on the basis precipitation rate, liquid water and stability; each phase was about eight hours in duration. Some potential for cloud seeding was present during the first two phases, when there was large liquid water and relatively warm cloud tops (-10 to -15^{o}C). Most of the precipitation (75 percent) fell over a nine-hour period during frontal passage; this amount also represented 10 percent of the total project snowfall.

ACKNOWLEDGEMENTS

We would like to acknowledge the contributions of all the project participants for obtaining the field observations in a difficult working environment. We appreciate their efforts in reducing the data and making it available for analysis and for assisting us with data interpretation.

M. Haurwitz assisted with the computer analysis of radiometer data, L. McCall drafted the final figures for this report, and J. Davis typed the manuscript.

TABLE OF CONTENTS

I. INTRODUCTION

A. Project Overview

In 1982, the Basic Design Plan for the State of Utah, under the cooperative federal and state program, outlined a research procedure for superimposing a research component on top of the Utah operational cloud seeding program (Grant and Mielke, 1982). The plan included objectives related to improved assessment of precipitation changes and to improvements in the technologies of remote sensing and cloud seeding. Several specific approaches were identified as vital to the research:

1. confirmation of the presence of supercooled liquid water
2. determination of the precipitation trajectories from natural and artificially induced snowfall
3. evaluating the effectiveness of the seeding material
4. determining ways to optimize the delivery of the seeding material

Resolution of these difficult objectives will provide the basis for making the Utah operational program more effective.

This research program has had three field seasons. The results of the 1981-82 season have been summarized in Hill (1982), and those for the 1982-83 season are in Long (1984). In earlier contributions by CSU, Rauber and Grant (1983; 1985) presented case studies andd showed that shallow orographic cloud systems in the Tushar data set accounted for a large fraction of the total project precipitation.

The present report summarizes analytical work at CSU which has concentrated on broad program objectives using the 1985 data set. This analysis extends our base of knowledge and places some of the results of the 1985 field work in the perspective of weather modification for the

Utah program. The analysis is important for interpreting the measurements obtained to describe the precipitation processes and can provide operational applications of the research. It also identifies particular courses of research that should be addressed in the next full scale field project.

B. Participants, Instruments and Data Sources

A list of participants and their contribution to the 1985 field research program is given in Table I. Swart (1985) gives a complete summary of the data collected during the eighteen STORM periods which were identified. A 'STORM' was distinguished in this project when there was significant cloud cover over the Tushar Mountains and when a time period was designated for intensive research activity (Long, 1984). Locations of instruments are shown on the project map in Figure 1. In 1985, the research field program was based in the Tushar Mountains and ran from January 15 through March 15.

Table I.

Participants in the 1984-5 field research program.

ORGANIZATION	CONTRIBUTION
Utah Divison of Water Resources (UDWR)	rawinsondes, precipitation gauges
Desert Research Institute (DRI)	scientific management
North American Weather Consultants (NAWC)	project coordination tracer experiment logistical support
National Center for Atmospheric Research (NCAR)	
Field Observing Facility Convective Storms Divison	C-band Doppler radar radio communications
National Oceanic and Atmospheric Administration (NOAA)	Ka-band Doppler radar
Wave Propagation Laboratory →	dual wavelength radiometer
University of Utah (UU)	LIDAR surface microphysics observations
Atmospherics Incorporated (AI)	supercooled liquid water detector

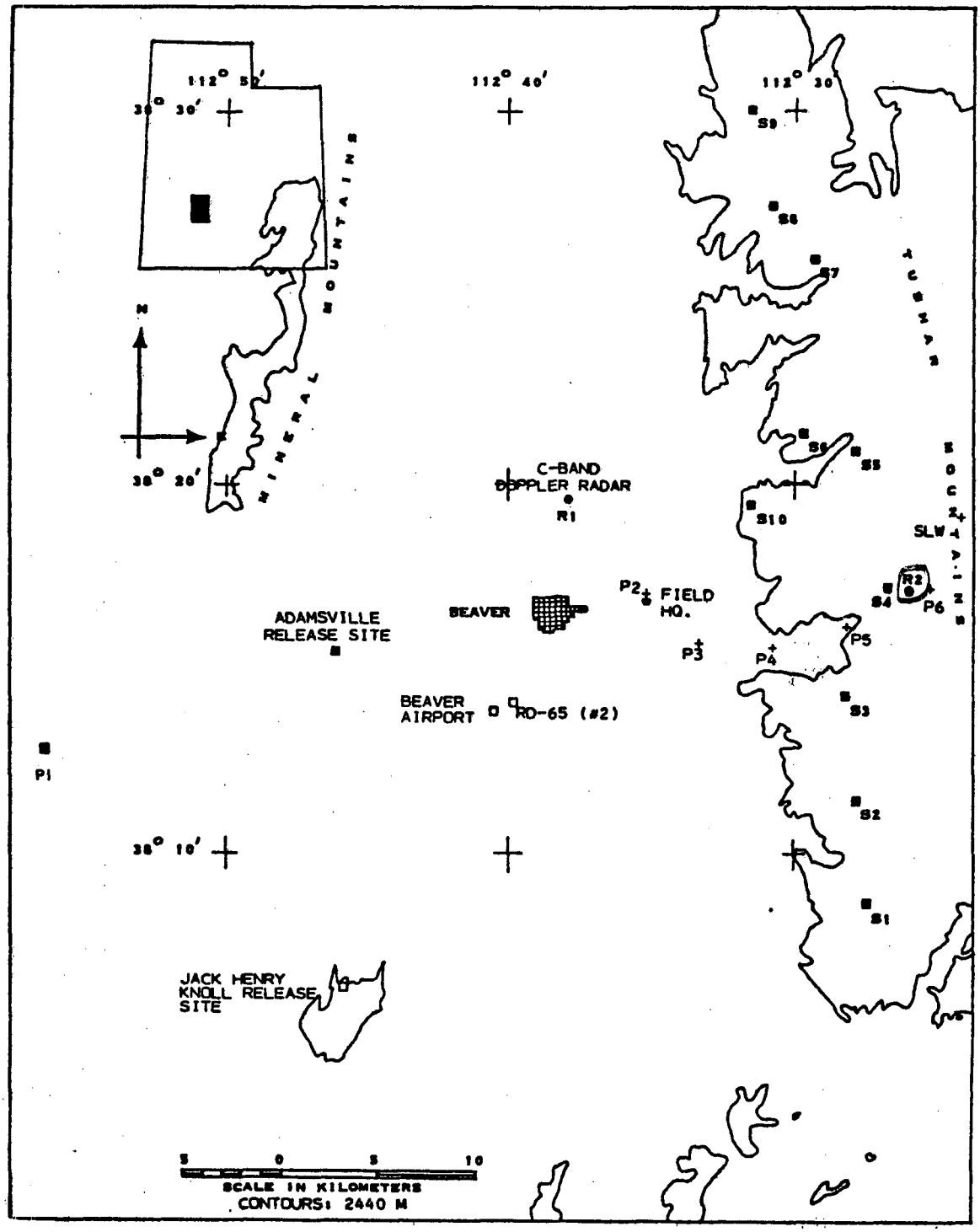

Figure 1. Map of project area showing the instrumentation network (taken from Swart, 1985). Terrain contour is 8000 ft MSL. P1 through P8 are time-resolved, recording precipitation gauges. S1 through S10 are snowpack sampling sites. The Ka-band radar, the radiometer, the LIDAR and surface ice crystal observations were based at the Merchant Valley site, R2. Rawinsondes were released from Adamsville.

C. CSU Research Tasks Identified

Two tasks were identified for CSU's research effort.

Task 1: Estimate of Maximum Modification Effect

At the 24 April 1985 meeting of the Utah/NOAA analysis participants, a desire to calculate precipitation efficiency was expressed. Due to the limitations imposed by a single rawinsonde upwind of the Tushars and a limited precipitation gauge network, calculation of precipitation efficiency in the thermodynamic sense of a water budget across the barrier could not be done. At that meeting, CSU proposed an alternative method which would relate more specifically to estimating the maximum effect attainable by appropriate seeding. The approach proposed was to calculate the flux of supercooled liquid across the mountain, using radiometer data and rawinsonde winds, and integrate this flux over each storm to determine the mass of liquid water crossing the mountain unutilized in the precipitation process. CSU agreed to perform these calculations in a correspondence with Dr. Long (8 May 1985). The results of this task are summarized in Chapter II.

Task 2: Case Study Analysis

CSU's research interest and commitment included a case study analysis of a STORM from the 1985 data set. The objective was to assemble a case study description of one storm event by integrating and intercomparing measurements from a variety of observations. Some unanticipated additional effort was required in reducing the Ka-band radar data -- Rochelle Blumenstein worked about three weeks on NCAR's RDSS in Boulder. The case study of STORM 9 is given in Chapter III.

II. ESTIMATE OF MAXIMUM POSSIBLE WEATHER MODIFICATION EFFECT

In this Chapter, an estimate of the total mass of liquid water which passes over the Tushar range, but is not utilized in the precipitation process, is determined by integrating radiometer data and rawinsonde winds during each storm. Two assumptions were necessary to perform these calculations:

but the rad. meter was upwind often in & scanning mode.

1. The values of liquid observed by the radiometer are representative of those along the crest of the mountain over the region where seeding would be effective (assumed in these calculations to be 50 km in north-south extent).
2. The cross-barrier component of the 700 mb wind speed is representative of the speed at which all of the liquid is passing over the mountain.

The approach used was to determine the average liquid water measured by the radiometer over a three-hour period centered on the launch time of each project rawinsonde. Since the radiometer was operated in two modes (zenith and scanning), an averaging scheme which accounted for both modes had to be developed. The averaging was done in the following way:

1. For each project variable, the radiometer data were checked for data availability. If radiometer data were available for any part of the three-hour period centered on the rawinsonde launch time, the data were used in the calculations.
2. The radiometer scanning data were normalized to the vertical.
3. The radiometer mean liquid water depth for the three-hour period was determined by the following equation:

$$\overline{LW} = \frac{\Delta t_Z \sum_{n=1}^{N_Z} LW_{Zn} + \Delta t \sum_{n=1}^{N_S} LW_{Sn}}{N_Z \Delta t_Z + N_S \Delta t_S} \quad (1)$$

where

$\overline{LW}$ is the average integrated liquid during the period

Δt_Z = 60 s, the averaging time for one liquid measurement in the zenith mode

Δt_S = 5 s, the averaging time for one liquid measurement in scan mode

LW_Z = a single measurement of liquid in the zenith sampling mode

LW_S = a single measurement of liquid in the scan sampling mode, normalized to the vertical component

N_Z = total number of measurements in the zenith mode

N_S = total number of measurements in scan mode

This value of liquid water was then used in the following equation to determine the volume, V, of supercooled water passing over the mountain in time interval, Δt:

$$V = \overline{LW}\, U_{700}\, Y\, \Delta t \quad (2)$$

where

U_{700} is the cross-barrier wind speed at 700 mb, and Y is the length along the mountain where a seeding effect is presumed to occur, assumed to be 50 km (the north-south extent of the terrain above 8000 feet). If $\overline{LW}$ is in mm, U_{700} in m/s, $Y = 5 \times 10^4$ m and $\Delta t = 1.08 \times 10^4$ s, the equation to retrieve V in acre-feet is

$$V \text{ (acre-feet)} = 437.8 \times \overline{LW} \times U_{700} \quad (3)$$

V, $\overline{LW}$, and U_{700} were determined for each period when simultaneous rawinsonde and radiometer data were available. The individual values of these variables for each rawinsonde launch are summarized in Table II. The data were also compiled for each STORM and are summarized in Table III.

Rawinsonde and radiometer data were available for different parts of each declared storm period. Nearly all data loss occurred during storms 1-4 when the radiometer was not operating. Of the 235 declared storm hours during the field season, 135 hours had data available. During this time period, an estimated 13,018 acre feet of water passed over the Tushars along a 50 km length of the mountain. Nearly half of this liquid passed over the mountain during one 30 hour event (STORM 9). STORM 15 contributed about one-fifth of the total. The remaining part was distributed among nine storms. Three storms had virtually no liquid measured during their lifetime.

A cumulative frequency histogram was constructed from the three-hour liquid water flux data in Table II and is shown in Figure 2. Notice that 50 percent of the project total is represented by the largest five periods of three-hour flux. Five of the six largest values occurred during STORM 9. It is clear that an effective weather modification effort must be able to anticipate the few time periods of high supercooled liquid water and treat them accordingly.

Values of the liquid water flux were also plotted versus 700 mb temperature in Figure 3. It shows that large values of liquid water flux were associated with 700 mb temperatures warmer than $-7^{\circ}C$. Although the true temperature distribution of the liquid water is not known, the trend shown here is consistent with cloud physics and weather

Table II

Liquid Water Flux Over The Tushar Mountains For
All Rawinsonde Launches During 1985 Field Program

Rawinsonde Time (GMT)	Rawinsonde Date	3 Hour Average Liquid Water Depth (mm)	U_{700} (ms)	Liquid Water Volume (Acre Feet)	Storm #
18	1/7/85	No data	--	No data	--
02	1/8/85	No data	--	No data	--
14	1/8/85	No data	--	No data	--
00	1/21/85	No data	--	No data	--
09	1/21/85	No data	--	No data	--
12	1/21/85	No data	--	No data	1
15	1/21/85	No data	--	No data	1
18	1/21/85	No data	--	No data	1
03	1/22/85	No data	--	No data	1
16	1/23/85	No data	--	No data	--
15	1/24/85	No data	--	No data	--
00	1/25/85	No data	--	No data	--
03	1/25/85	No data	--	No data	--
00	1/26/85	No data	--	No data	--
12	1/26/85	No data	--	No data	--
15	1/26/85	No data	--	No data	2
18	1/26/85	No data	--	No data	2
21	1/26/85	No data	--	No data	2
00	1/27/85	No data	--	No data	2
03	1/27/85	No data	--	No data	2
06	1/27/85	No data	--	No data	2
09	1/27/85	No data	--	No data	2
12	1/27/85	No data	--	No data	--
15	1/27/85	No data	--	No data	--
18	1/27/85	No data	--	No data	--
18	1/28/85	No data	--	No data	3
21	1/28/85	No data	--	No data	3
00	1/29/85	No data	--	No data	3
03	1/29/85	No data	--	No data	3
06	1/29/85	No data	--	No data	3
09	1/29/85	No data	--	No data	3
12	1/29/85	No data	--	No data	3
18	1/30/85	No data	--	No data	4
03	2/2/85	0.000	--	0.0	5
12	2/2/85	0.052	9.8	224.2	5
15	2/2/85	0.043	10.0	188.2	5
00	2/3/85	0.015	4.5	29.7	5
03	2/3/85	0.050	4.3	94.5	5
17	2/3/85	0.018	6.1	48.0	6
00	2/4/85	0.030	6.0	78.1	6
04	2/4/85	0.055	6.7	161.1	7

Table II (Cont.)

Rawinsonde Time (GMT)	Rawinsonde Date	3 Hour Average Liquid Water Depth (mm)	U_{700} (ms)	Liquid Water Volume (Acre Feet)	Storm #
12	2/4/85	0.000	--	0.0	7
15	2/4/85	0.000	--	0.0	7
18	2/4/85	0.000	--	0.0	7
01	2/6/85	0.000	--	0.0	--
21	2/7/85	0.000	--	0.0	8
00	2/8/85	0.000	--	0.0	8
03	2/8/85	0.015	11.3	73.9	8
06	2/8/85	0.036	11.3	178.4	8
12	2/8/85	0.000	--	0.0	9
15	2/8/85	0.000	--	0.0	9
00	2/9/85	0.273	10.0	1190.1	9
03	2/9/85	0.236	8.3	862.5	9
06	2/9/85	0.052	10.9	247.4	9
09	2/9/85	0.227	12.7	1265.8	9
12	2/9/85	0.232	11.3	1150.5	9
15	2/9/85	0.275	9.9	1195.2	9
18	2/9/85	0.206	3.5	312.9	9
00	2/10/85	0.010	3.8	16.7	9
03	2/10/85	0.000	--	0.0	9
17	2/12/85	0.062	10.5	285.8	10
13	2/20/85	0.000	--	--	11
18	2/20/85	0.036	5.2	82.6	11
21	2/20/85	0.006	0.2	0.6	11
00	2/21/85	0.000	--	0.0	11
01	2/23/85	0.004	3.2	5.7	12
17	2/23/85	0.000	--	0.0	--
21	2/25/85	0.000	--	0.0	--
06	3/2/85	0.000	--	0.0	--
12	3/2/85	0.000	--	0.0	--
19	3/2/85	0.007	-2.3	0.0	13
03	3/3/85	0.006	7.3	19.2	13
06	3/3/85	0.055	12.3	296.1	13
09	3/3/85	0.065	9.3	265.4	13
12	3/3/85	0.005	6.2	13.6	13
15	3/3/85	0.000	--	0.0	13
18	3/3/85	0.000	--	0.0	13
21	3/3/85	0.000	--	0.0	13
09	3/7/85	0.000	--	0.0	--
00	3/8/85	0.061	8.1	215.2	14
03	3/8/85	0.016	11.9	83.3	14
14	3/10/85	Bad data	--	--	15

Table II (Cont.)

Rawinsonde Time (GMT)	Rawinsonde Date	3 Hour Average Liquid Water Depth (mm)	U_{700} (ms)	Liquid Water Volume (Acre Feet)	Storm #
21	3/10/85	0.484	8.5	1794.3	15
00	3/11/85	0.120	12.2	638.7	15
06	3/11/85	0.062	6.7	181.3	--
12	3/11/85	0.001	6.9	3.0	--
18	3/12/85	0.174	-1.4	0.0	16
00	3/12/85	0.009	-1.1	0.0	16
06	3/12/85	0.329	4.4	637.9	17
09	3/12/85	0.198	9.3	801.6	17
17	3/12/85	0.102	7.2	321.4	18
23	3/12/85	0.021	6.7	61.3	18
22	3/18/85	No data	--	No data	--
06	3/19/85	No data	--	No data	--
14	3/19/85	No data	--	No data	--

Total # of rawinsondes: 94
Total # of rawinsondes when radiometer data available: 57
Total # of rawinsondes when average LWC $\geq$ 0.01 mm: 31
Total # of rawinsondes when average LWC $\geq$ 0.05 mm: 21
Total # of rawinsondes when average LWC $\geq$ 0.10 mm: 12

Table III

Amount of Liquid Water Passing Over Barrier Crest
Along 50 km Length During Each STORM

STORM No.	Period of STORM (hr:min)	Period of Observation (hr:min)	Percent of STORM Observed	Liquid Water (acre ft)	Corrected Liquid Water (acre ft)
1	14:50	0	0	--	--
2	17:10	0	0	--	--
3	18:50	0	0	--	--
4	6:35	0	0	--	--
5	23:25	15:00	64	536	838
6	7:45	6:00	77	126	164
7	9:20	9:00	96	0	0
8	7:50	7:50	100	252	252
9	31:20	31:20	100	6235 = 48%	6235
10	2:20	2:20	100	286	286
11	12:10	10:30	86	83	97
12	8:40	3:00	35	6	16
13	29:05	20:30	69	594	861
14	10:20	6:00	58	298	514
15	13:20	6:00	45	2431	5403
16	5:40	5:40	100	0	0
17	6:55	6:00	87	1443 (14)	1659
18	10:50	6:00	55	383	696
Non Storm Periods		27:00		345	345
Total	236:25	135:10	58	13018	
Projected total if all storms were observed 100%					17366

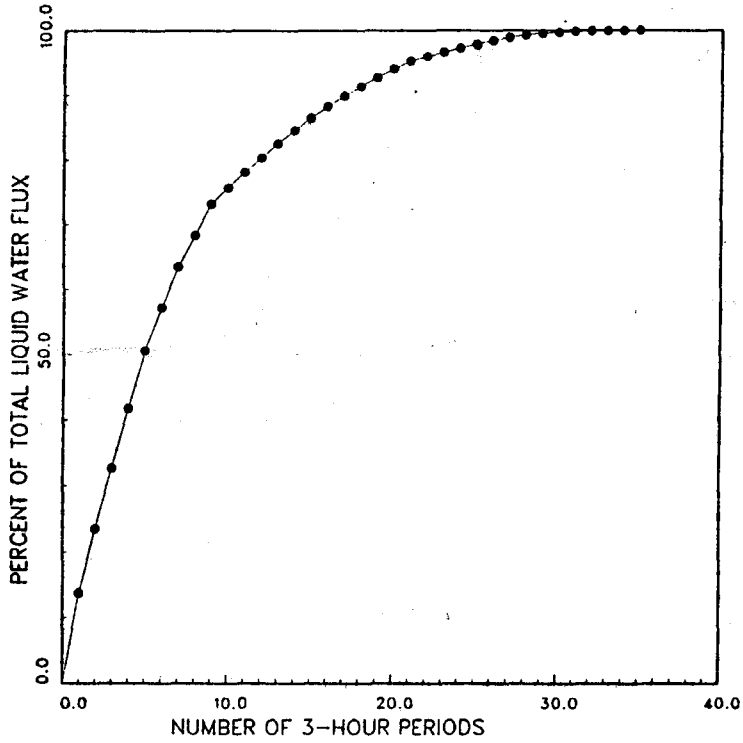

Figure 2. Cumulative frequency distribution showing the percent of liquid water flux for 35 three hour periods during the 1985 research season, 15 January to 15 March. Values are ranked by percent.

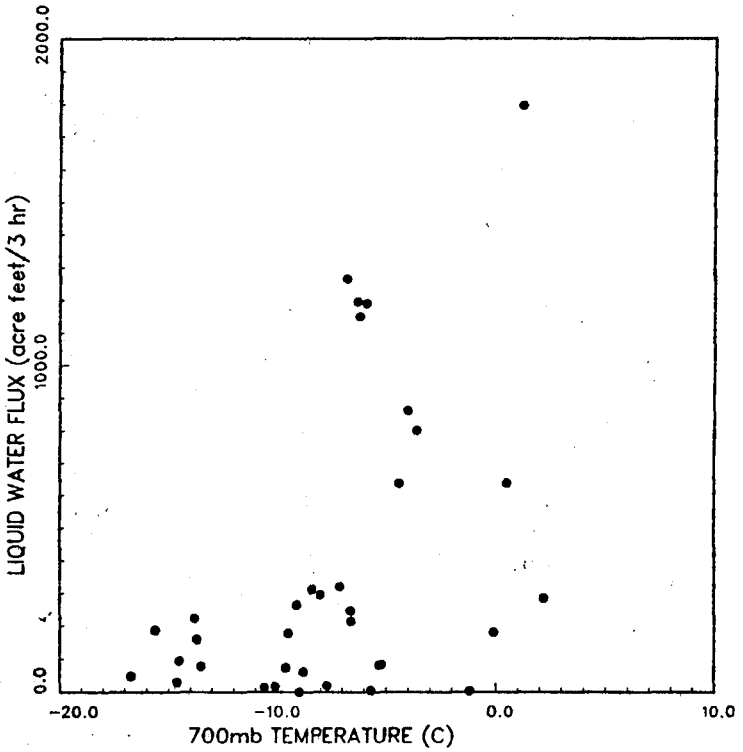

Figure 3. Liquid water flux for 35 three hour periods during 1985 research season versus 700 mb temperature from Adamsville rawinsondes.

modification concepts: at temperatures warmer than about -10°C, the concentration of natural ice nuclei is very small, so that ice phase precipitation mechanisms are inefficient, and large values of liquid water are observed.

Figure 4 shows the relationship between the liquid water flux data and the simultaneous precipitation rate, as given by averaging the data from the eight project precipitation gauges, there is no apparent correlation of precipitation rate and liquid water flux. Some storm periods had naturally high precipitation efficiency (values having low water flux and high precipitation rate), while others were inefficient (high water flux and low precipitation rate). Generally speaking, the warmer periods shown in Figure 3 had less efficient precipitation processes, as indicated by relatively large liquid water flux and small precipitation rate.

If one assumes that the periods when rawinsonde data were not available for each storm had characteristics similar to the periods when rawinsonde data were available, an estimate of the total amount of water passing over the mountain during the 1.5 month project period can be obtained (excluding the first four storms). The projected total of liquid passing over the Tushar range if all storms were observed for their duration was 17,366 acre feet.

If weather modification efforts were able to (1) convert this supercooled water to ice, (2) have 100 percent of this converted water arrive on the ground as precipitation, and (3) not reduce the amount of natural ice which would have arrived at the ground without modification, the net effect would be an increase in snow available for runoff by about 17,000 acre feet. These assumptions are unrealistic--it is more

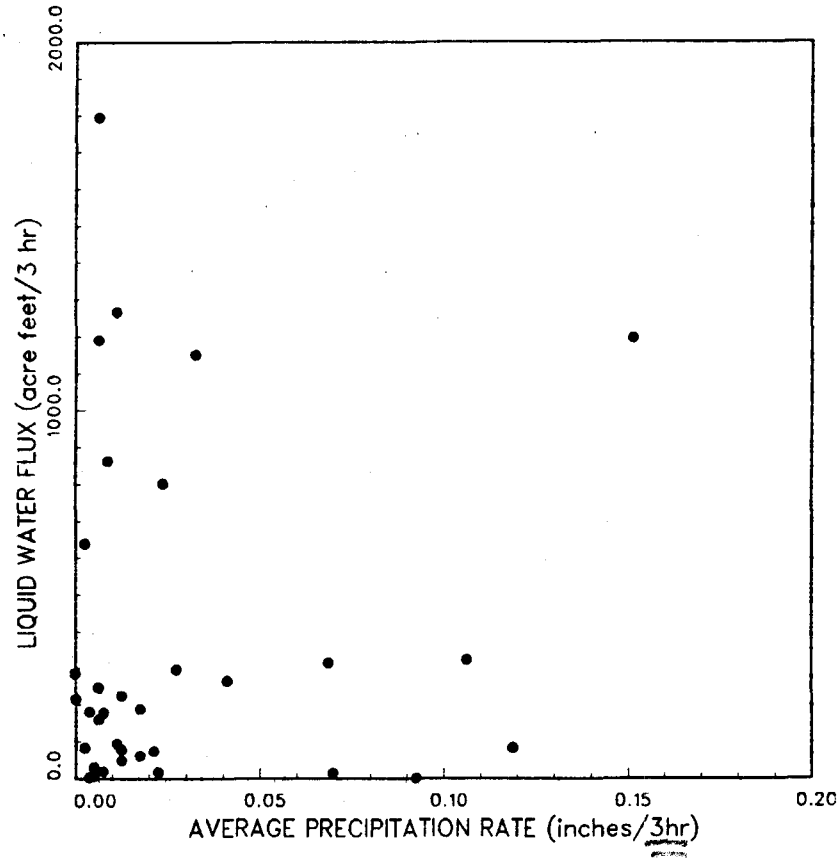

Figure 4. Liquid water flux for 35 three hour periods during 1985 research season versus simultaneous precipitation rate in the Tushar Mountains, as given by averaging the eight recording gauges.

likely that only a fraction of this amount could be realized.

To put this value in perspective, consider it in terms of the average 70 year annual runoff for the Beaver River (which drains the target area) -- 38,250 acre feet. Cloud seeding during appropriate periods of storms with the ideal conditions described above and with 100 percent efficiency would have produced a 45 percent increase over the natural runoff. $\frac{13018}{38250} = 34\%$

III. CASE STUDY STORM - FEBRUARY 8-9, 1985

A. Overview

The objective of this analysis was to assemble a case study description of one STORM event and to intercompare the observations that were obtained in order to arrive at a better understanding of the precipitation formation processes and the potential for cloud seeding opportunities. A large variety of measurements were made, including: dual wavelength radiometer, Ka-band radar, C-band radar, rawinsondes, surface observations of precipitation type and amount, LIDAR, and the icing probe.

The February 8-9 STORM was a large scale cold frontal system which went through several different phases of structure and precipitation processes. The additional orographic component could not be readily differentiated from the large scale storm. This one STORM provided about 13 percent of the total precipitation during the two-month project. Some positive potential for cloud seeding was likely because considerable supercooled liquid water was present during both light and heavy precipitation periods, and cloud temperatures were generally in the range -5 to -20°C.

Four phases of this STORM were distinguished, based on static stability, precipitation intensity and the amount of liquid water:

Phase I. February 8, 1330 - 2100 (MST)
stable, stratified with layered clouds
little precipitation and moderate amounts of
supercooled liquid water

Phase II. February 8, 2100 - 0400 February 9
convectively unstable with little precipitation
and slight liquid water

Phase III. February 9, 0400 - 1300
convectively unstable, heavy precipitation from deep
clouds accompanying cold frontal passage,
moderate liquid water

Phase IV. February 9, 1300 - 2100
stable, light precipitation, dissipating stage

In the following sections of this report, the overall STORM structure and chronology will be described first. Then a detailed account will be given for each of the four phases.

B. Synoptic Summary

This STORM was an upper level short wave that moved across the western states from the northwest. The 500 mb map is shown in Figure 5 at the time the surface cold front passed the project site in Utah. It shows a weak short wave (note 12 hour height changes of only about 50m), propagating through a broad, flat long wave trough located over the western United States. The short wave moved relatively slow, about 10 miles per hour at 40 degrees north latitude. Thermal advection at 500 mb was weak until 00Z 9 February; in the next 12 hours, the temperature dropped from $-20^{o}C$ to $-25^{o}C$.

The surface weather map in Figure 6 shows that there were several frontal features during this time period. As is typical for this region during winter, the stationary cold front along the eastern side of the

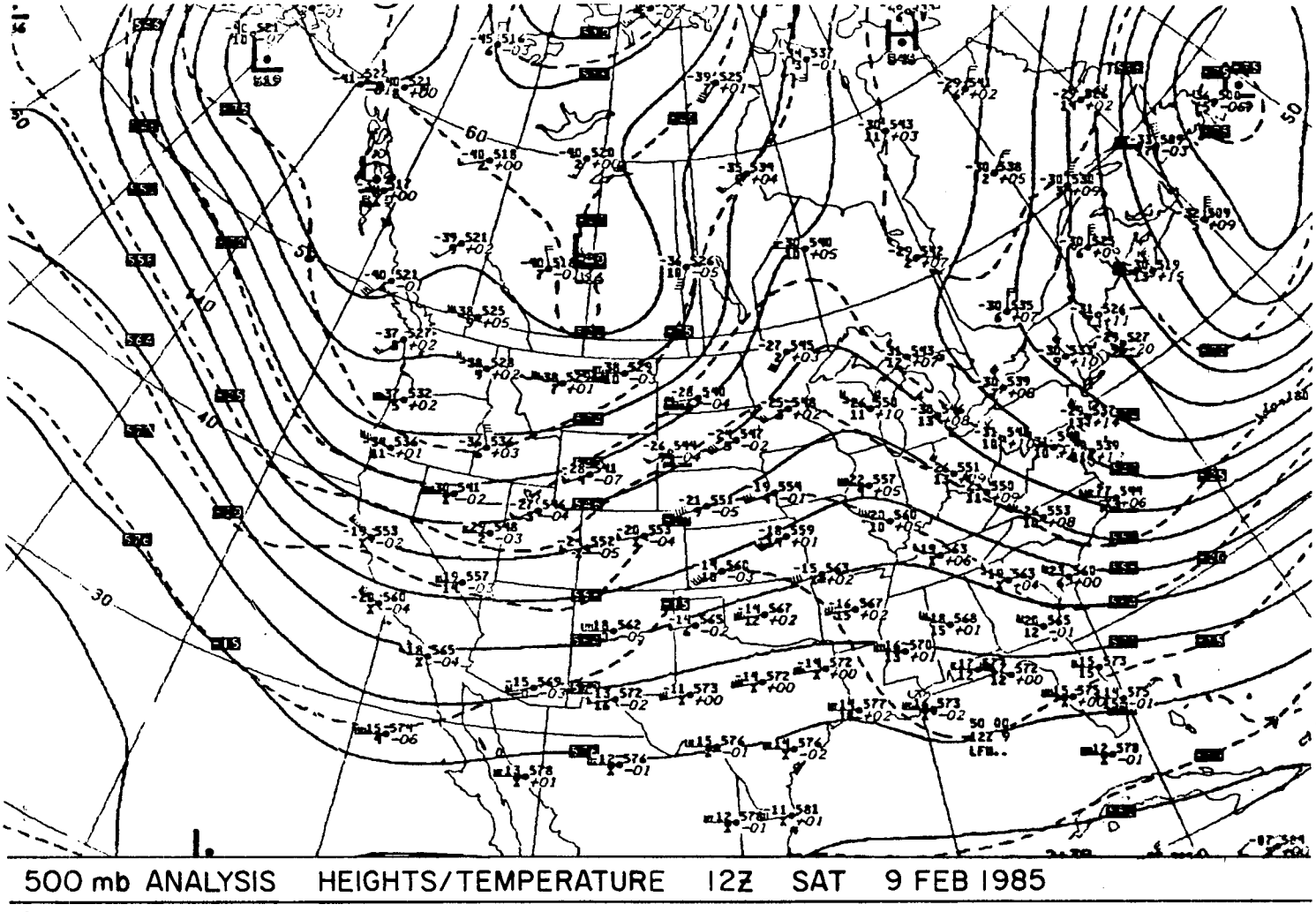

Figure 5. National Weather Service 500 mb analysis for 1200GMT, Saturday 9 February 1985.

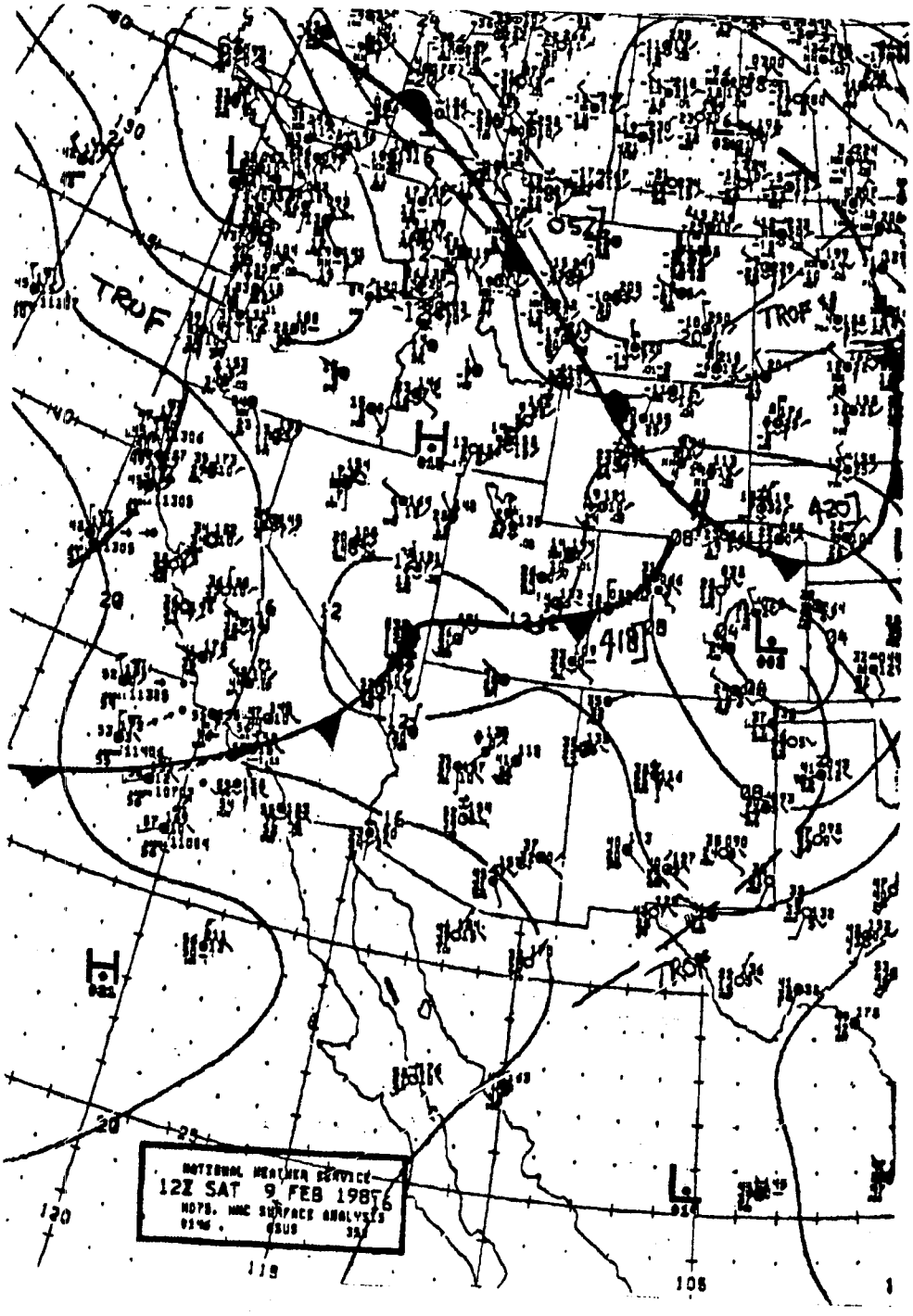

Figure 6. National Weather Service surface weather map analysis for 1200GMT, Saturday 9 February 1985.

Rockies had been present for several days or more. A fresh outbreak of Arctic air was moving southeast across the Great Plains, and it reached into northern Texas 24 hours after this time. None of this cold air reached west of the eastern front range of the Rockies into Utah. Cyclogenesis ahead of the upper trough began as lee troughing in eastern Colorado 24 hours previously. At the time of these maps, the surface cylone was split between the older low in southern Nevada and the developing one in eastern Colorado. Notice that the upper level flow was nearly parallel with the surface cold front in Utah. Consequently, after this time the Utah cold front moved only a little further south and began to weaken as the upper level support was transfered east of the mountains.

The surface cold front passed the project site at about the time of these maps and was accompanied by heavy snowfall for several hours.

Figure 7 shows an atmospheric cross section of equivalent potential temperature that was constructed from the rawinsonde observations taken at the Adamsville site. The location of the cold frontal surface was determined from the wind shift boundary. The significant feature related to the precipitation for this STORM is the layer of convectively neutral or unstable air. It begins in the lowest 100 mb 22 hours before frontal passage and becomes elevated and extends to about 6 hours after frontal passage. This neutral/unstable layer at low levels has been identified as a characteristic of the early stages in orographic storms in Colorado's San Juan mountains (Cooper and Saunders, 1980). However, the lowest level blocked flow that was found there is not present here. The greatest convective instability occurred from eight hours before to one hour after frontal passage. Notice that there was a shallow (ca. 50

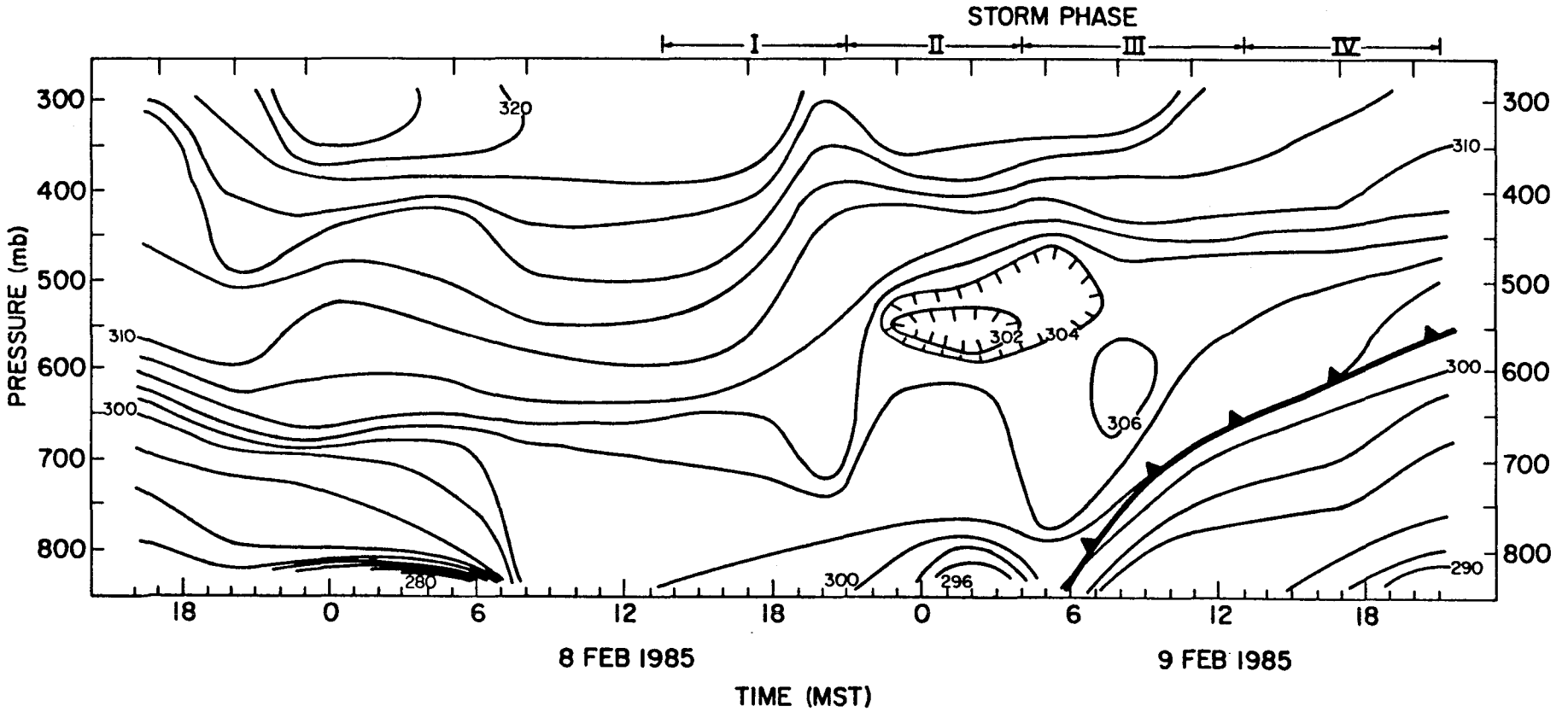

Figure 7. Atmospheric cross section of equivalent potential temperature (deg K), derived from Adamsville rawinsondes. Times of rawinsondes are shown by tic marks at top. STORM phases are delineated. Cold front surface is also shown.

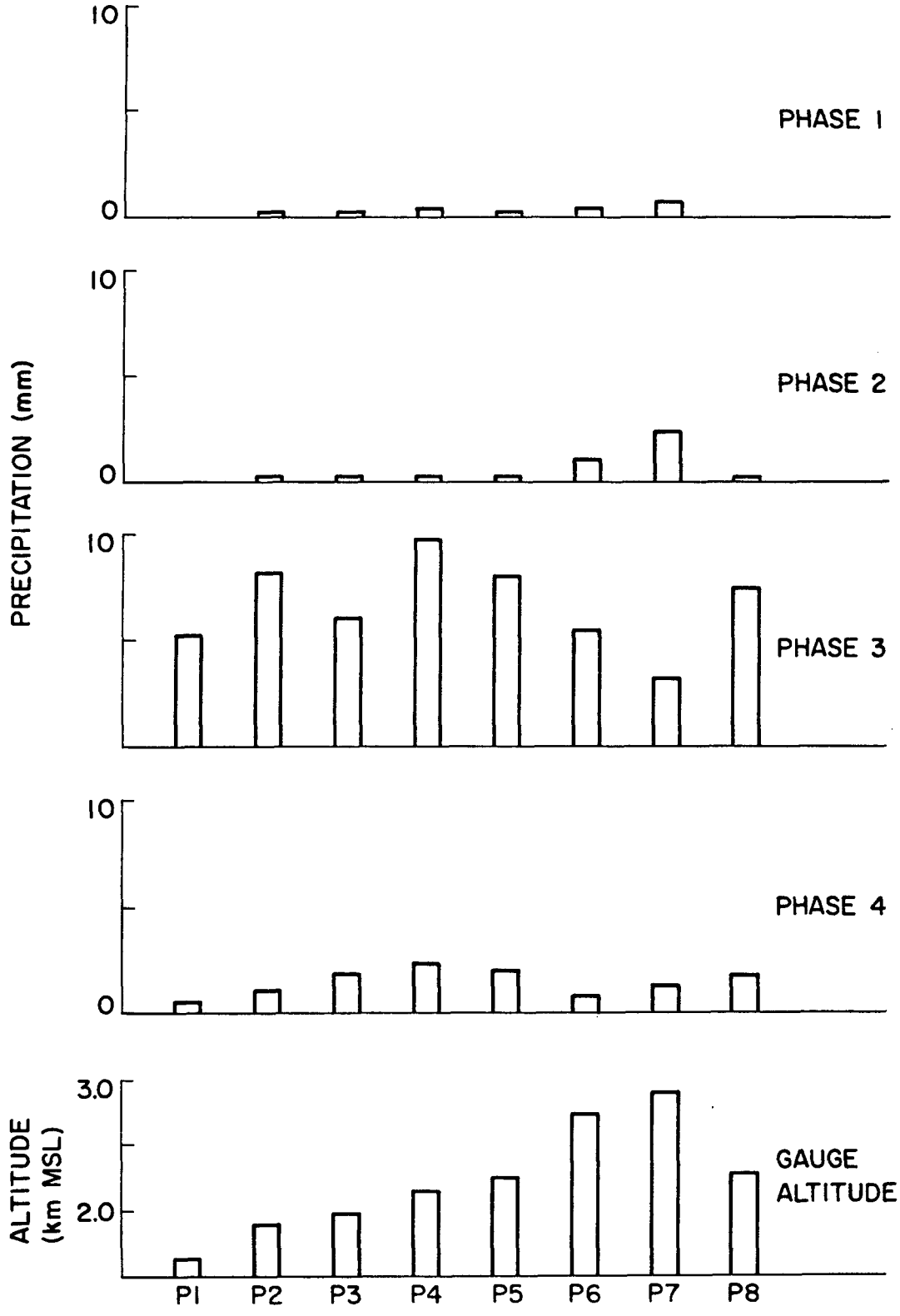

Figure 8. Precipitation history for the eight recording gauges. Gauge altitude is also shown (bottom) and suggests the terrain profile along west (left) to east (right).

mb thick) stable layer capping the instability; this stable layer defined the top of convective clouds and progressed from low, warm altitudes to higher, colder altitudes. The cross section also shows that before the STORM period, there was a low altitude, stable cold air drainage flow which was present at the Adamsville site in the Beaver basin after sunset and lasting until about sunrise on February 8. Winds in this drainage flow were from the southeast, with southwesterlies above. The drainage flow was about 25 mb thick (250 m). another low level stable cold layer was present on the following night. It had winds from the southwest and was probably not a simple drainage flow.

Throughout the STORM, the rawinsonde observations indicated that in the Beaver Valley, airflow was from the southwest to west at all altitudes except in the cold airmass, where it backed to northerlies. Typical wind speeds at 700 mb were 10 to 15 m/s and at 500 mb, 15 to 20 m/s.

C. STORM Description

Precipitation amounts were averaged for the eight project gauges (Swart, 1985) during each of the four STORM periods, and the values are plotted in Figure 8. The figure also shows gauge altitude for reference. Recall from Figure 1 that gauge #1 is at a valley site about 30 km west of the Tushar Mountains, and the others cross the mountain range. Gauge #8 is on the lee side of the Tushars for westerly flow, and gauges #6 and #7 are at high altitude locations. Figure 8 shows that most of the STORM precipitation occurred during phase III. Furthermore, the spatial distribution of snowfall was not "orographic'" during this phase, as the amounts do not follow the terrain profile. In contrast, phases I and

II show strong orographic effects. Thus we conclude that most of the precipitation from this STORM was not orographically induced, but was caused by storm-scale dynamical forcing. A cloud seeding approach premised on orographic cloud physics would be appropriate only during the early phases of this storm.

A variety of data from this STORM were condensed and are presented as a chronology in Figure 9. Justification for dividing the STORM into four phases is provided in this figure and in the atmospheric cross section (Figure 7). One of the important characteristics of this STORM was that the heavy precipitation was concentrated into about 1/10 of the total STORM duration. The cold front passage in the Beaver Valley occurred at 0600, and most of the precipitation fell during phase III in association with the front. The top panel shows the precipitation rate measured by the University of Utah observer who collected and weighed 15 minute samples at the Merchant Valley site (Fukuta and Winther, 1985). The large variability during phase III is probably a combination of sampling uncertainty and the large spatial and temporal changes in convective snowfall. In the second panel from the top, the 30 minute precipitation values from the eight recording gauges were averaged; for each gauge, the resolution is 0.01 inches in 30 minutes, or approximately 0.5 mm/hr. It appears that these two measurements of precipitation rate would be in substantial agreement if the data in the top panel were smoothed.

The cloud top temperature in the third panel of Figure 9 was derived from the vertical cross sections of the Merchant Valley Ka-band radar data (VAD analysis of the Doppler signal) and Adamsville rawindsonde soundings. The fourth panel shows radiometer liquid water

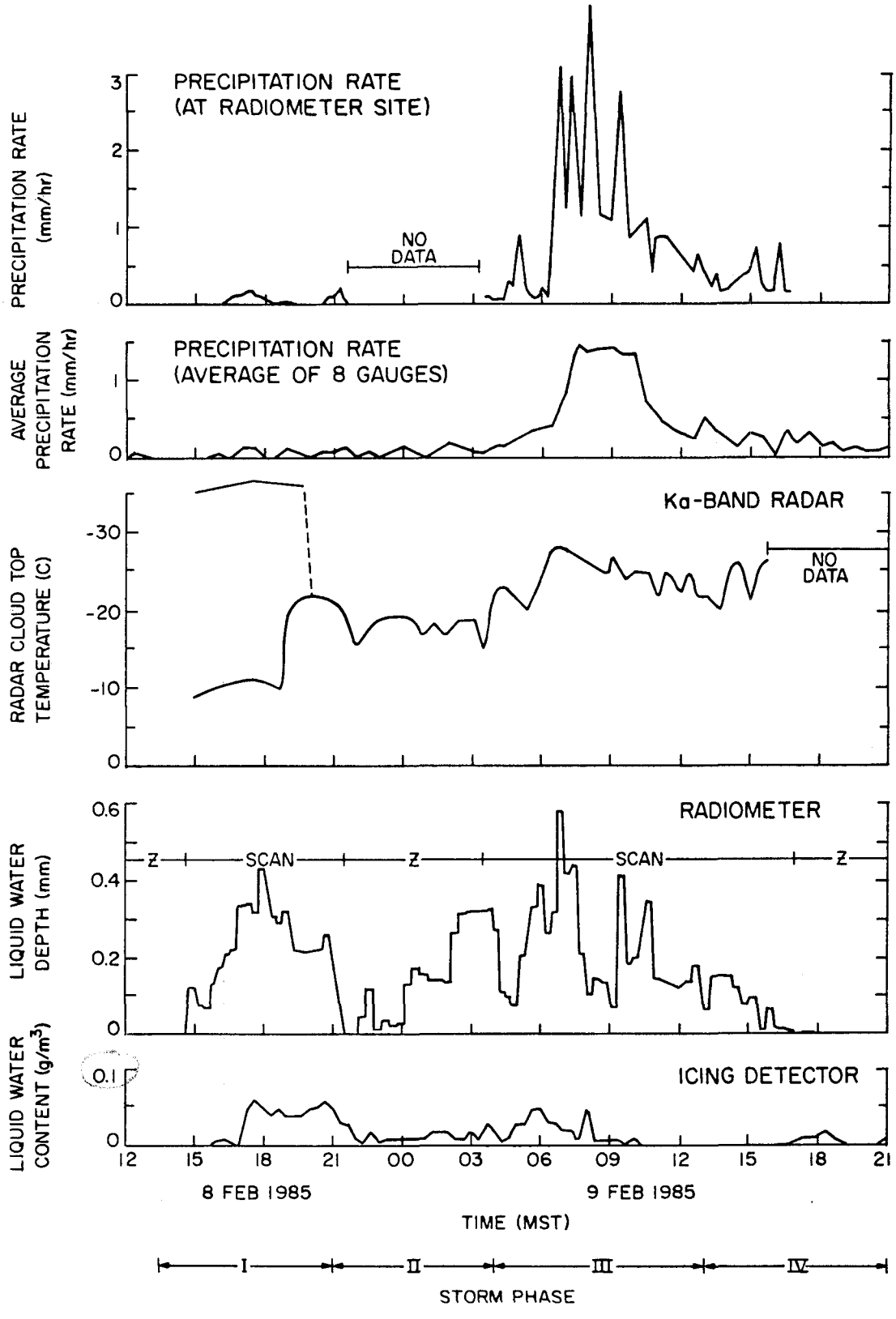

Figure 9. Chronological summary of STORM 9 from a selected set of data.

data averaged over approximately 20 minute periods: during scan mode, one azimuth-averaged value was plotted for each complete scan, which takes about 20 minutes; and during zenith mode, the data were averaged for 20 minutes to be approximately consistent with the scan data. Two cloud top temperatures are plotted during phase I because the radar indicated two separate layers. The thick cirrus layer probably had high ice concentrations and no liquid water because of its cold temperature, and conversely, the low stratus cloud probably had low ice concentration and contained the bulk of the liquid water detected by the radiometer. Apparently the cirrus layer was not seeding the warm stratus below, because the precipitation rates were small even though there was considerable liquid water. As phase I ended, the cirrus cloud dissipated and left altocumulus with tops slightly warmer than $-20^{o}C$. This was apparently not cold enough for significant precipitation to develop in phase II. When the deep convection of phase III began, cloud tops rose to $-25^{o}C$, and with the abundant liquid water, precipitation was heavy. In the final phase of the STORM, both liquid water and precipitation dissipated.

The bottom panel in Figure 9 shows surface measurements of supercooled liquid water which were obtained with a Rosemount icing detector located near the crest of the Tushar Mountains (Solak and Allen, 1985). During the first half of the STORM, the trend of this liquid water measurement was consistent with the Merchant Valley radiometer data; travel time from Merchant Valley to the ridge was about 20 minutes. However, during the later, heavy precipitation periods, the low altitude liquid water was relatively less. This is consistent with the expectation that the low altitude liquid water was strongly depleted

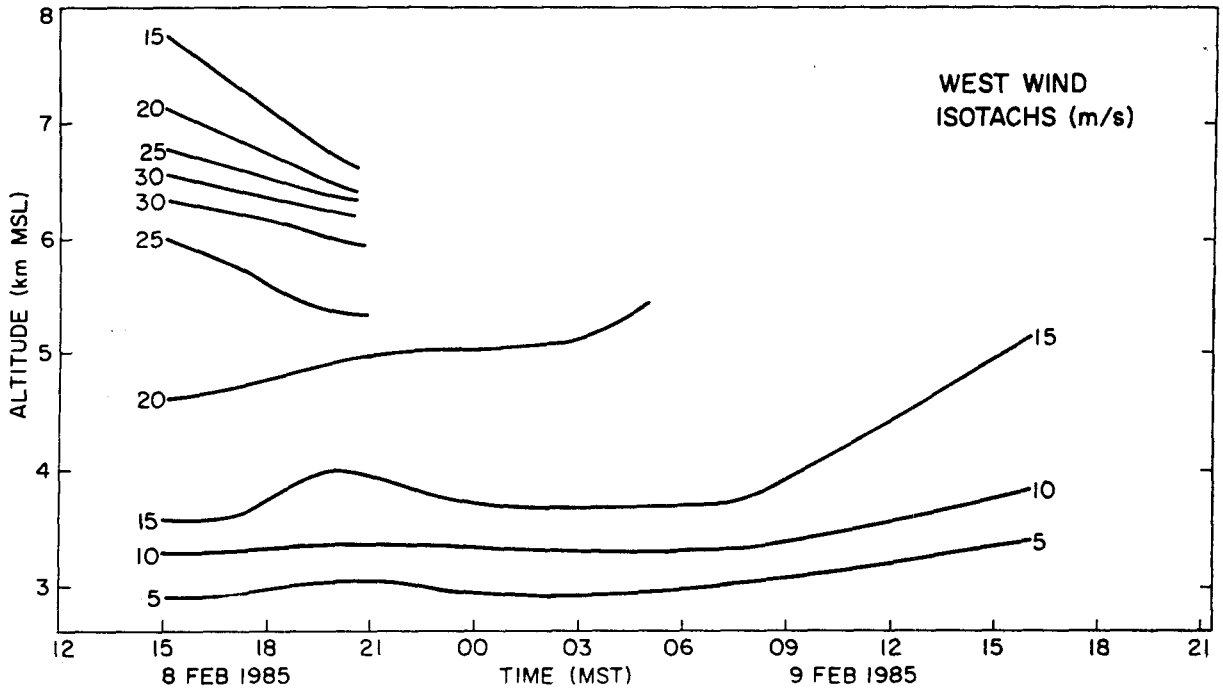

Figure 10a. Westerly component of the horizontal wind for STORM 9 derived from three hour averages of Ka-band Doppler radar data at Merchant Valley.

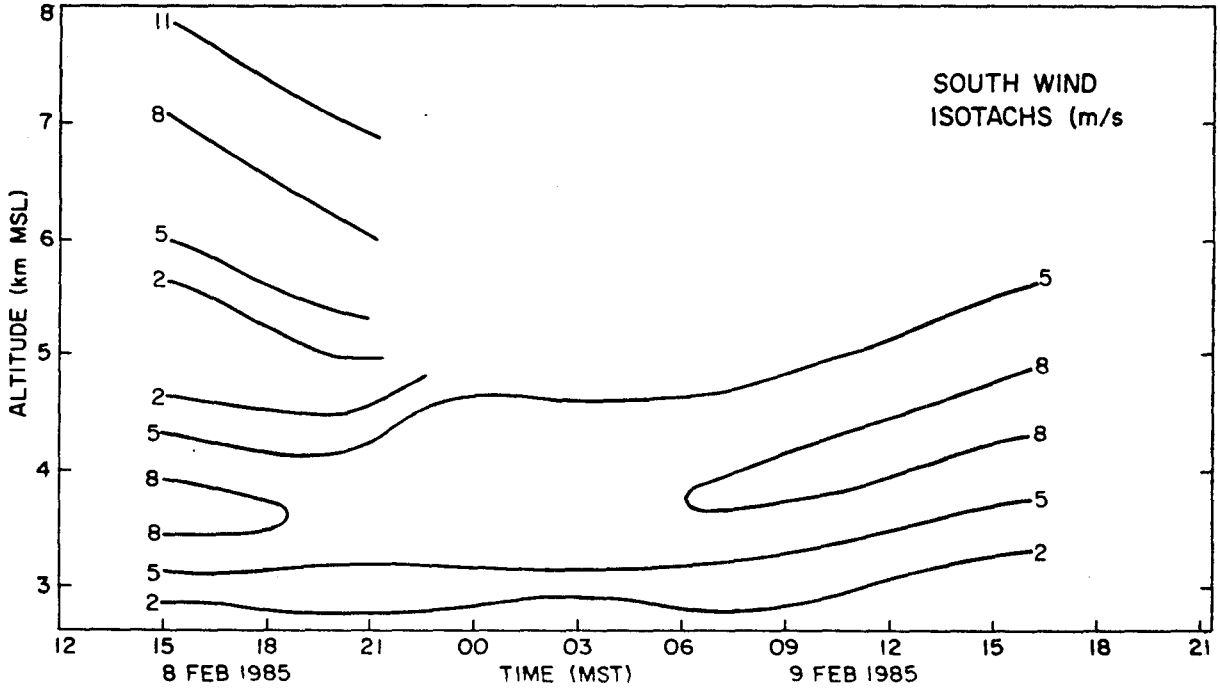

Figure 10b. Southerly component of the horizontal wind for STORM 9 derived from three hour averages of Ka-band Doppler radar data at Merchant Valley.

by diffusional and accretional growth of precipitation particles falling through the cloud.

The history of horizontal winds is shown in Figures 10a and 10b for the Merchant Valley location. This figure was derived from Doppler velocity data from the NOAA Ka-band radar; they used the VAD analysis technique with 70 degree elevation angle. Minimum detectable radar reflectivity was about -30 dBz. Doppler data are not available below this reflectivity threshold. The figures show that the winds were relatively constant over the Merchant Valley site throughout the STORM. The similar history derived from the Adamsville rawinsondes is different in two respects. First, the cold frontal passage was prominent at 0600 MST February 9 at Adamsville; it had the classical wind shift from southerly to northerly components. But the front was virtually unidentifiable in the winds over Merchant Valley. We surmise that the cold airmass was not deep enough and did not have enough momentum to reach the Merchant Valley altitude (800 m higher than Beaver). Second, low level wind speeds from the two sites are not in agreement relative to height above sea level, although they do agree relative to height above ground. Apparently the valley and mountain had similar boundary layer depths of about 1 km. The shear in the boundary layer was moderate, 0.01 per second. The C-band radar, which was located in the Beaver Valley, should provide more detailed information on these differences. Because of the consistency in the winds over the Merchant Valley location it is possible to cite 'typical' values for the altitude range where most of the precipitation formed: 3, 4 and 5 km (MSL) as 230° 6m/s, 246° 18m/s, and 260° 20m/s, respectively.

Figure 11 is a repeat of Figure 4 with the data points for STORM 9

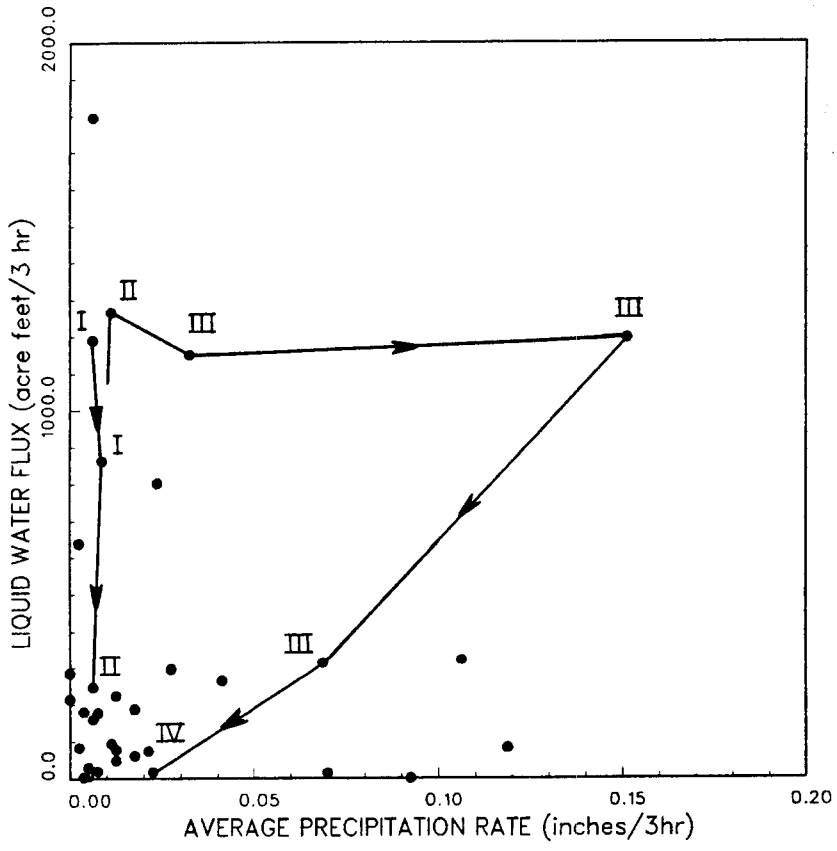

Figure 11. Liquid water flux for 35 three hour periods during 1985 research season versus simultaneous precipitation rate in the Tushar Mountains, as given by averaging the eight recording gauges. Lines connect values from STORM 9 in chronological order, with STORM phase indicated.

connected in chronological order to show the sequence of liquid water flux and precipitation. Early in the STORM (phases I and II), there were relatively large amounts of liquid water flux but small precipitation rates, indicating relatively inefficient precipitation processes. Later (phase III), there were increases in precipitation rate while the liquid water flux remained large and steady. This period might be characterized as having moderate efficiency. Finally (phase IV), the liquid water flux and precipitation rate both declined as the STORM dissipated. According to this figure, STORM 9 was most efficient during its final stages. Reasons for the changes in precipitation amounts and efficiencies will be explored in the next section, which has detailed descriptions of the separate phases of this STORM.

D. STORM Phases

PHASE I

Phase I of this STORM is shown in Figure 12 in a format similar to Figure 9, as a chronology of observations. The top panel shows the vertical history of Ka-band radar reflectivity at Merchant Valley. NOAA produced these data using VAD analysis with 70 degree elevation angle; the vertical resolution is 66 m. VAD scans were taken at 10 minute intervals. The reflectivity values are averages over a circle in each range gate. At 5 km MSL, the circle is 1.7 km diameter. Minimum detectable radar reflectivity was about -30 dB; the -10 dB contour was chosen to be the minimum in this figure. Isotherms from the Adamsville rawinsonde observations are superimposed on the radar reflectivity profiles. The second panel from the top shows precipitation histories from each of the eight recording gauges. The third panel shows

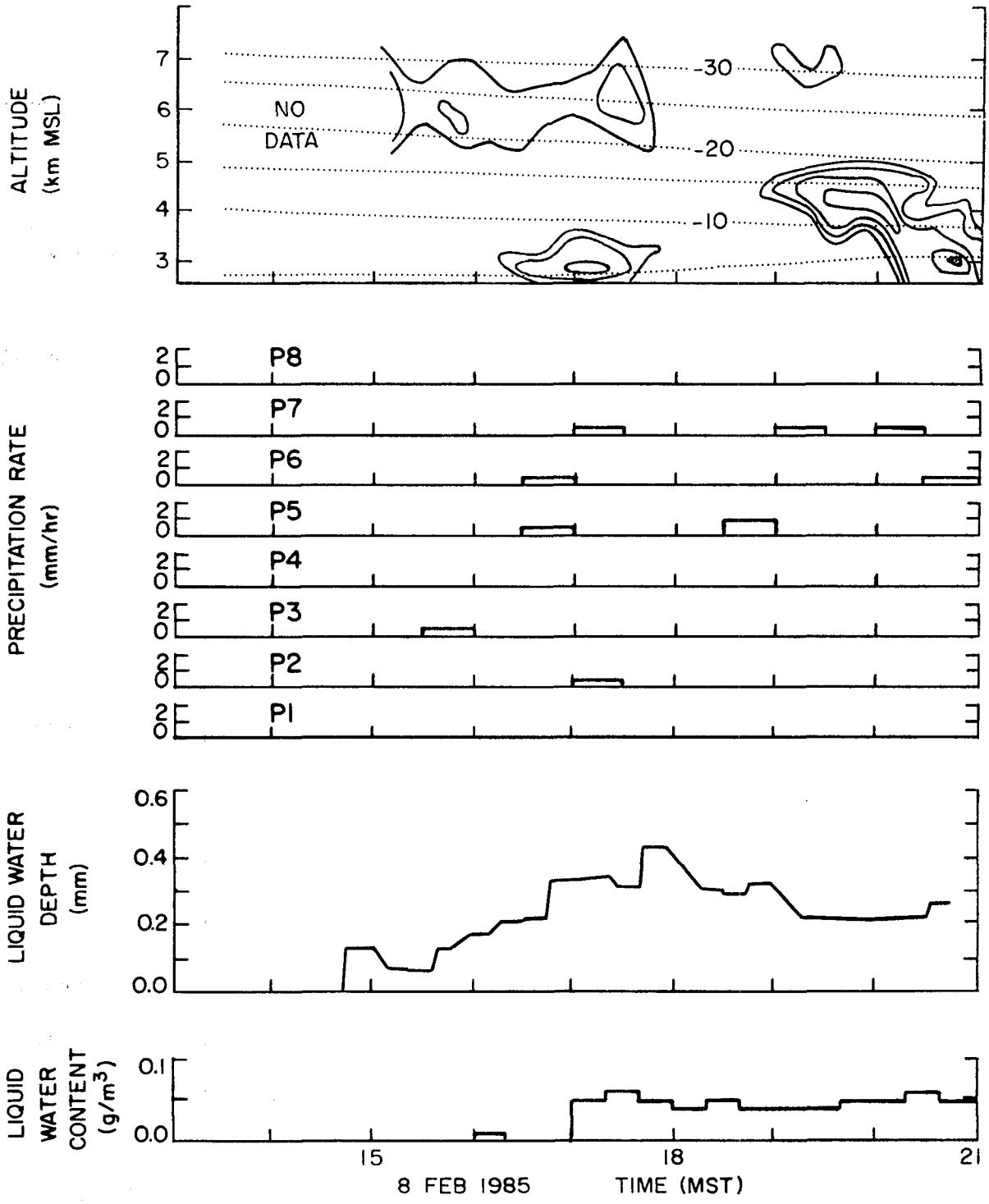

Figure 12. Chronology of Phase I as given by a selected set of observations. Time-height Ka-band radar reflectivity (top) contours start at -10 dB and increment by 5 dB. Precipitation data from the eight recording gauges (second panel). Radiometric liquid water depth (third panel from top) values show either an average for a complete scan (in scan mode) or average over 20 minutes (in zenith mode), as appropriate. This phase had only scan data. Liquid water content (bottom panel) shows surface measurements from Rosemount icing probe.

radiometer data averaged over the approximate 20 minute periods, as in Figure 9. During scan mode, one average value was plotted for each complete scan, which represents about 80 observations and takes about 20 minutes. To calculate the average, the values were weighted by the normalized width of the azimuth angle that the value represents. For zenith mode data, averaging was done for 20 minutes to be approximately consistent with this presentation of the scan data. The bottom panel shows measurements from the icing probe.

The beginning of the STORM had intermittent snowfall of light intensity. LIDAR observations at the Merchant Valley site showed the water cloud base descending from about 3.3 km at 1400 to 2.8 km at 1600 (Sassen, 1986). It stayed at 2.8 km for the remainder of phase I. Ice crystals at the surface from 1600 to 1800 (MST) fell from what appears to be a single convective element. The crystals were small, single graupelized snow particles showing moderate to heavy riming. Temperatures in the lower cloud were -5 to $-10^{o}C$, where column and needle type crystals grow (Magono and Lee, 1966); significantly, no crystals of this habit were observed at the surface. The data suggest that some of the precipitating ice crystals from the thick, cold cirrus cloud were probably seeding the liquid water cloud below. The relatively large values of liquid water at the surface and aloft suggest that this seeding was not in sufficient concentrations to provide an efficient precipitation process. From 1800 to 2000, no significant snowfall was observed at the surface, which is consistent with the Ka-band radar and LIDAR data. From 2000 to 2100, another convective element moved over the area and produced light precipitation of rimed dendrites and aggregates. Again, the surface observations are consistent with the cloud structure

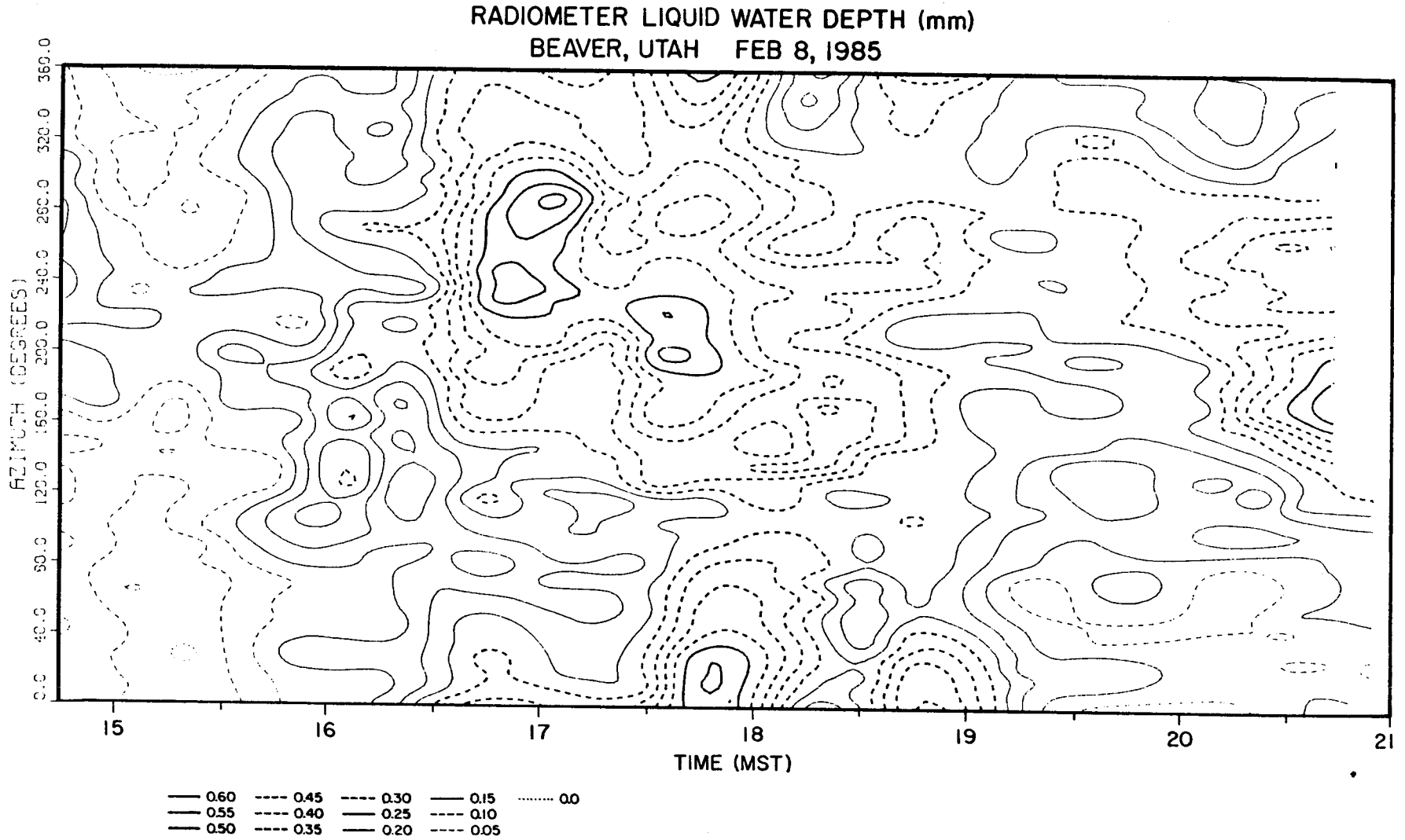

Figure 13. Contour plot of liquid water depth derived from NOAA dual channel radiometer operating in scan mode during STORM phase I.

defined by the radar, the radiometer and the LIDAR.

The NOAA dual wavelength radiometer was operated in scan mode during phase I of the STORM. Figure 13 is a contour plot of the radiometric liquid water, shown as a time and azimuth diagram. The raw data comprise an irregular skewed grid, since the radiometer begins scanning clockwise from azimuth 120 degrees and finishes one scan after about 17 minutes. It then rewinds counterclockwise for about 3 minutes, taking no data, and starts a new scan. This plot was constructed by finding the vertical comdponent of liquid water and then interpolating these values to a rectangular grid. The contours were determined by computer analysis. The histories of the liquid water in Figure 12 and Figure 13 are from the same data, but the contour plot gives a more complete description. The large values in liquid water at 1700 were associated with air in the upwind quadrant, southwest to northwest from the radiometer, and the peak at about 1800 represents two areas of liquid water, one to the north and the other, south-southwest. We have suggested that this phase of the STORM showed orographic effects, but the radiometer data indicate this was not a cloud having uniform, homogeneous or steady liquid water which is usually thought to characterize stable orographic clouds. Also, the liquid water does not show a maximum over the main ridge of the mountains to the east, which would be expected for a predominantly orographic cloud. The hydrographic divide is approximately 8 km from the radiometer and occupies the entire eastern semicircle. Apparently the western first rise of the Tushar range, 10 km west of the Merchant Valley site, was the major barrier causing lift in this case. In order to justify constructing contours of the data, we must presume that atmospheric features persisted longer

than the 20 minutes between successive scans at the same azimuth and that they were relatively homogeneous over distances larger than about 20 km (17 m/s wind X 20 minutes). The data neither support nor refute these assumptions. Aircraft measurements in other orographic clouds suggest that there is often considerable fine scale structure (of the order 1 km in size) and that many liquid water features are not steady (e.g., Rauber and Grant, 1985).

Toward the end of this phase, the cirrus cloud dissipated and the stable layer above 3 km MSL was being lifted and was weakening. This destabilization continued through the second and third phases of the STORM.

PHASE II

The chronological summary for phase II is shown in Figure 14. Observations of this phase were biased by operational considerations. That is, many of the project personnel stopped to eat and sleep during the night. For the most part, there were no LIDAR measurements and no surface crystal observations; the radiometer was put in zenith mode for unattended operation. The available evidence indicates this phase was a period of relatively steady, light precipitation. The vertical history of Ka-band radar data shows cloud tops were confined below 4.5 km, and stayed warmer than $-17^{o}C$. The transient radar features were approximately 20 minutes apart. These features were associated with slightly heavier snowfall at the site, for example, from 2300 to midnight. The transition to heavy precipitation in phase III is seen in the last half hour; surface crystal samples at this time found heavily rimed dendrites. These data suggest that the crystals nucleated near

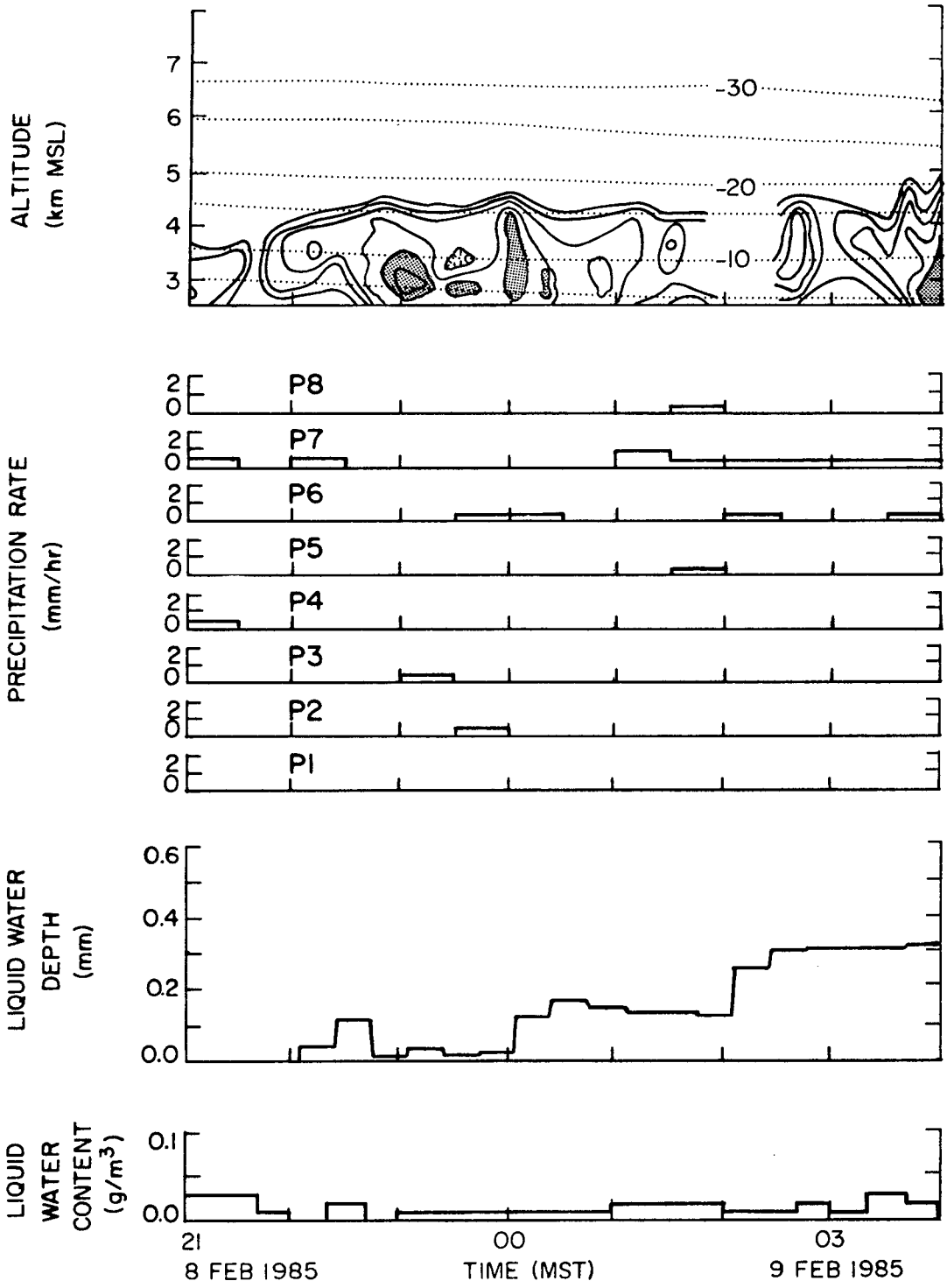

Figure 14. Similar to Figure 13, but for Phase II.

cloud top in small concentrations, grew by vapor diffusion in the -13 to -17°C temperature region and began accretional growth when their size exceeded the riming threshold size of about 200 um (D'Errico, 1978).

The liquid water traces in Figure 14 from the icing probe and the radiometer suggest that the cloud depth increased in a rather steady fashion through the seven hour period. This trend is shown to be somewhat misleading in Figure 15, where the twenty minute average values from Figure 14 are plotted on top of the one minute data from which the averages were calculated. It is apparent that there was considerable variation about the increasing trend. This kind of liquid water signal would be produced when a nearly solid altocumulus cloud is advected over the radiometer. The maxima in liquid water are associated with the rising air in embedded convection, and the minima are associated with the downdrafts. This picture of convection capped by a stable layer is consistent with the instability cross section (Figure 7). Spectral analysis was performed on the one minute data, and the power spectrum is shown in Figure 16. There are several peaks in the spectrum, notably at frequencies of 1/(12 minutes) and 1/(6 minutes). If we let the 4 km wind (18 m/s) represent the horizontal motion of the liquid water field, then the distance between convective elements would be about 13 km. Since the radar VAD analysis was done with 10 minute intervals, the radar display in Figure 14 cannot resolve the fine scale structure that the radiometer shows was there. However, RHI scans by the Ka-band radar have fine scale resolution, and they were done every 10 minutes along azimuth 070/250 degrees (parallel with the 4 km wind). One particular episode was chosen for closer comparison of the radiometer and RHI data, 0100 to 0130, because there were three prominent peaks in liquid water (cf.,

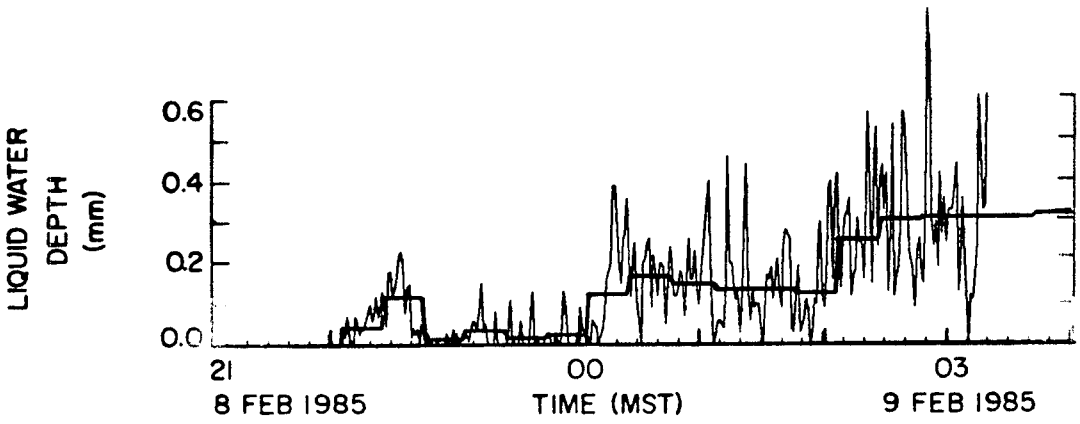

Figure 15. Liquid water depth derived from six hours of one minute resolution data from the NOAA dual channel radiometer operating in zenith pointing mode during STORM phase II, overlaid with the trace of 20 minute average values of the same data.

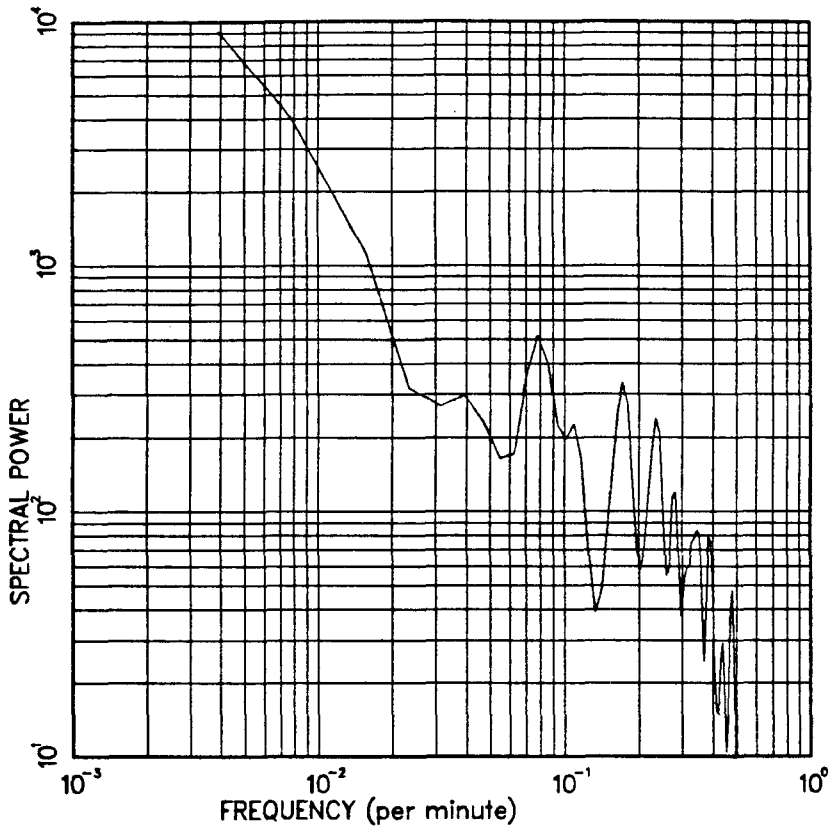

Figure 16. Spectral analysis of six hours of one minute resolution radiometer liquid water data in Figure 15.

Figure 15); these correspond with the 1/(12 minute) peak in the power spectrum. During this time period, the RHI scans showed elements of higher reflectivity which reached to cloud top. These elements were about 2 km in size and separation, which corresponds with the radiometer's spectral peak at 1/(6 minutes). The zenith radiometer data were overlayed on the RHI scans by transposing time and distance with the 4 km winds. Relative to the reflectivity maxima, the liquid water maxima were displaced about 1 minute later in time (or 1 km upwind). This description could be modelled as convective elements which are initially vertical and are tilted by the wind shear. The radar echoes then form first with the precipitation in the colder temperatures near cloud top. The liquid water persists longer at lower altitudes than at high altitudes because there is a lack of ice particles, and the wind shear separates the radar reflectivity and liquid water maxima. As the precipitation particles fall to lower altitudes, they could encounter either undepleted liquid water or no liquid water, depending on the spacing of convective elements, the magnitude of the wind shear, and the time to grow particles. The radar PPI displays showed more and higher reflectivity echoes were occuring north of the radar than south. Echo entities were about 5 km in size on the PPI. A more complete analysis of the fine scale nature of this cloud is warranted, and for this purpose, additional data reduction is required. This is not pursued in this report.

The low level stability during phase II suggests that ground based seeding may not have had a good chance for delivering the seeding agent to the liquid water cloud because the stable cold air in the Beaver Valley boundary layer (Figure 7) would not support vertical mixing.

mixing. Therefore, surface generators would have to be located above 750 mb (8000 ft) southwest of the Tushar Mountains. Factors which favor weather modification during phase II include the relatively warm cloud tops and continuing production of liquid water.

PHASE III

Figure 17 shows the chronological summary of phase III. We caution the reader that the vertical scale for the radar data has been exaggerated by a factor 2 relative to Figures 12 and 14. This was done so the time scale would be the same for all these figures. The reason for this adjustment is that the computer radar data analysis was performed with a time interval of 10 minutes for the phase I and phase II data, and 20 minutes for the phase III and IV data. The graphical analysis shown here was traced from a microfiche print of the computer graphical output, at which time the abscissa and ordinate plot scales were not independently adjustable.

In phase III the radar time-height cross-section became strongly convective in character, with radar cloud tops reaching 5.5 to 6 km and then descending to 4 km over a one hour time scale. With 20 m/s winds at 5 km, these convective elements were approximately 30 km in size. Radar reflectivities peaked at 15 dBz at low altitude and were associated with peaks in snowfall intensity, as shown by the data at gauges P5 and P6 which were near the radar site. This nine hour period contributed 75 percent of the STORM total precipitation.

The radiometer was operated in scan mode throughout phase III; at the time of this report, we did not have a time-azimuth plot of the scan data. In spite of the heavy precipitation, there was always excess

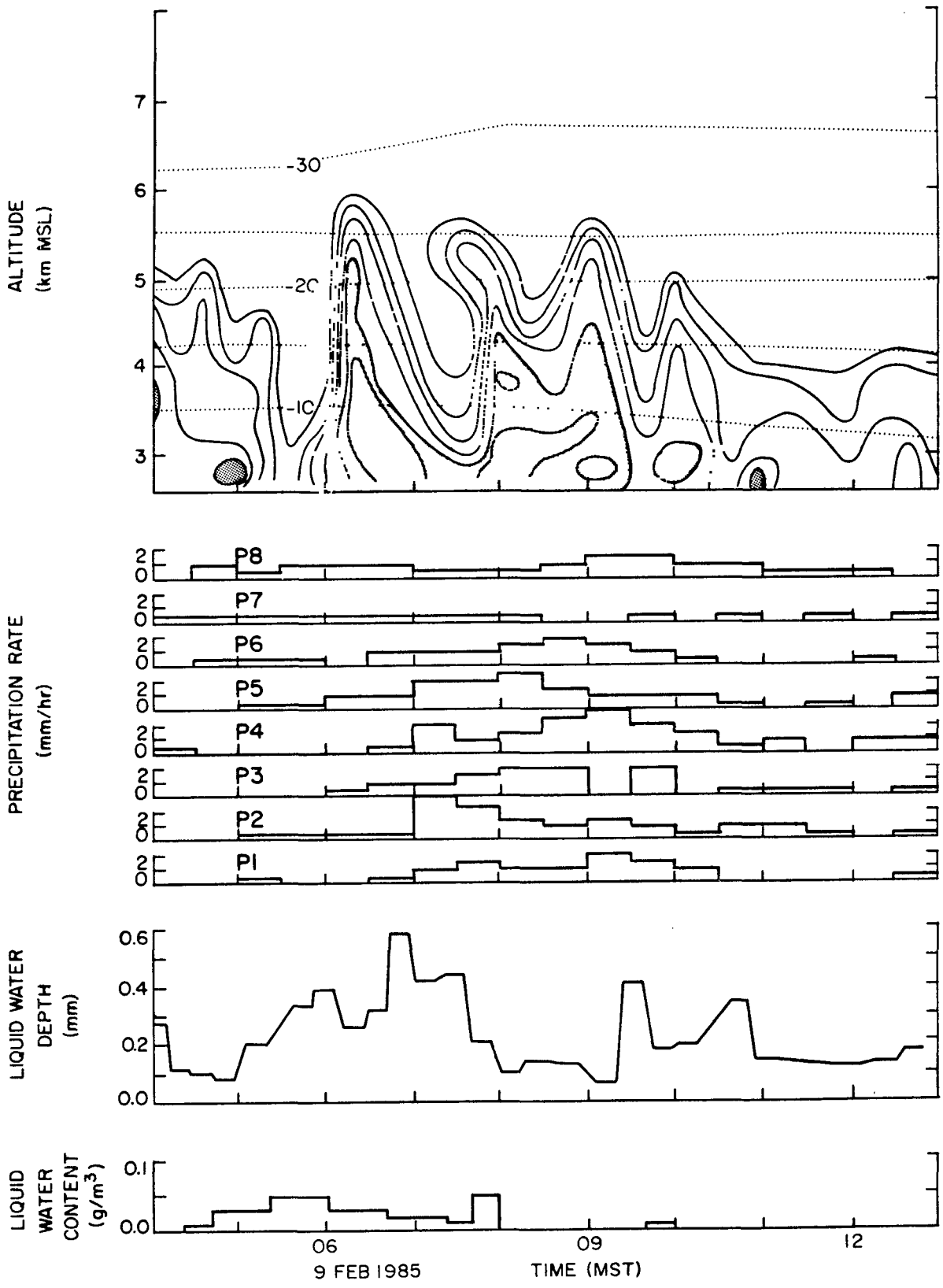

Figure 17. Similar to Figure 12, but for Phase III.

liquid water, which suggests that there may have been some potential for weather modification. With 18 m/s winds, there was still about 7 minutes travel time for the precipitation to include more of the liquid water since the Merchant Valley site is about 8 km from the barrier crest. It remains for future precipitation modeling studies to determine if this amount of liquid water would be consumed in precipitation growth in 7 minutes.

Before 1000, the precipitation could be described as heavily rimed single particles most of the time. This snowfall was occasionally so heavily rimed that it was described as graupel showers. There were two brief periods of aggregation snowfall, and they correspond with the times of largest radar reflectivities near the surface and with the heaviest precipitation rates, 0710 and 0820. The rimed single particles were of both dendritic and columnar habits. Ice crystals were growing by diffusion and riming throughout the depth of the cloud.

Cloud base was near the surface (2.6 km), according to LIDAR data, and radar cloud top was at about 5 km. If we assume the liquid water was uniformly distributed between these altitudes, then the average liquid water concentration in cloud was 0.04 g/m**3 at the minima and 0.3 g/m**3 at the maxima. These values are not unreasonable estimates. Future precipitation modelling studies should try to determine if this amount of liquid water would be consumed by the observed crystals in 7 minutes travel time to the barrier.

After 1100, there was a reduction in the amount of riming. Large dendritic crystals were predominant, and they formed large aggregates. The radar time-height cross section shows the convective period was ending. Precipitation was becoming light and less variable.

PHASE IV

Figure 18 shows the chronological summary of phase IV. As for Figure 17, the vertical scale for the radar data has been exaggerated by a factor 2 relative to Figures 12 and 14. This phase of the STORM was characterized by light, relatively steady precipitation with little change in precipitation type. The reduction in the amount of riming continued after phase III. Large, unrimed dendritic crystals predominated, and there was some aggregation. No crystal observations were made after 1700. The radar data are also incomplete, but they, together with the precipitation gauge data, suggest that the deep convective period was over.

The radiometer was operated in scan mode from 1300 to 1700, and then in zenith mode. At the time of this report, we did not have a time-azimuth plot of the scan data. The radiometer liquid water trend shows a steady decrease over the first three hours, reaching zero just after 1600. Before 1600, there was excess liquid water, and there may have been some potential for weather modification. The LIDAR data showed the cloud base was near the surface. If we assume the liquid water was uniformly distributed between the base and the radar cloud top at 4.4 km, then the average liquid water concentration in cloud was a maximum 0.08 g/m**3. Precipitation modelling studies should determine if this amount of liquid water would be consumed in precipitation growth before reaching the barrier. The liquid water trace from the surface icing probe is quite different from the radiometer. The absence of liquid water before 1700 could indicate that the precipitating dendritic crystals were consuming the low altitude liquid water. There is

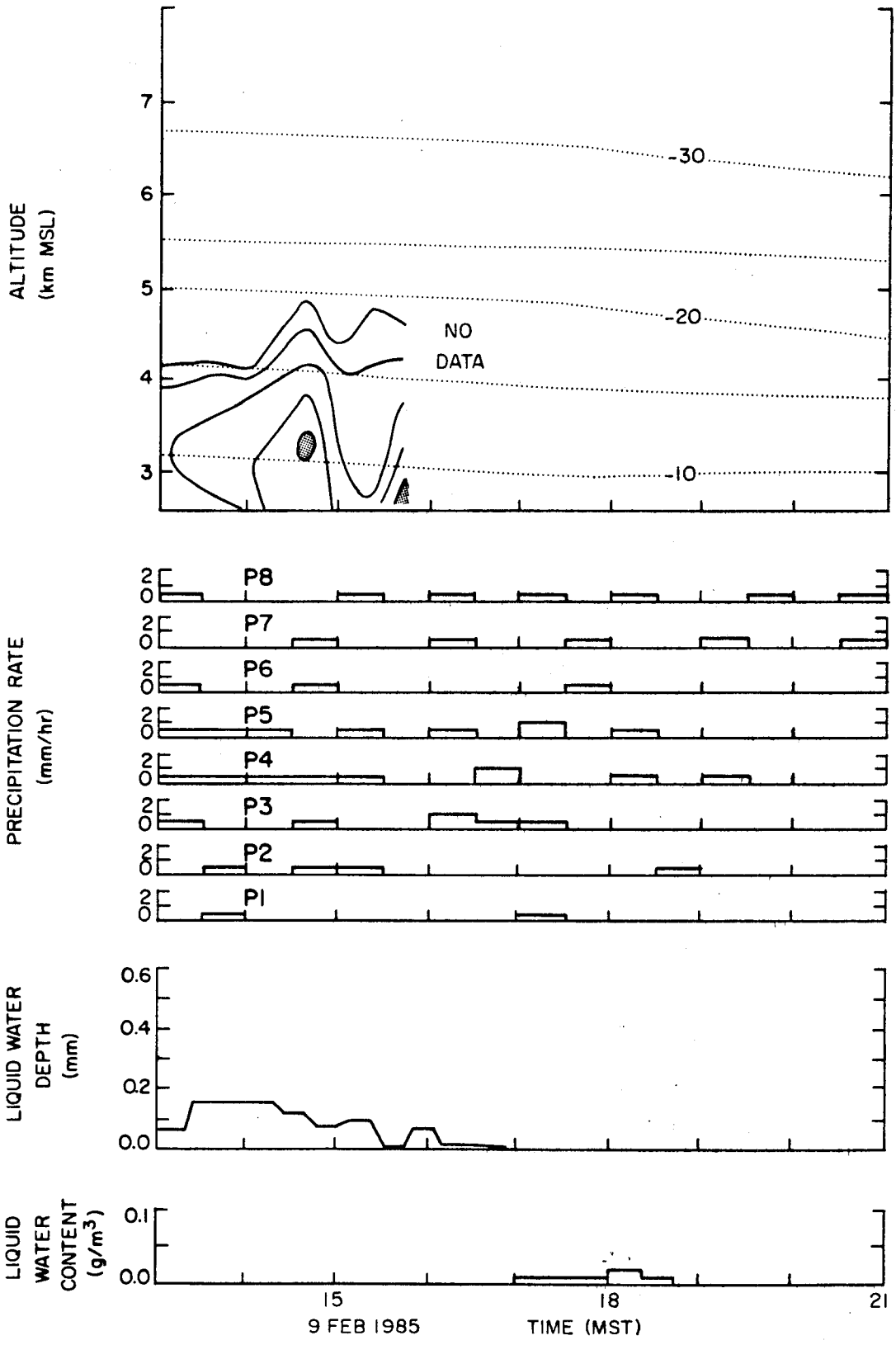

Figure 18. Similar to Figure 12, but for Phase IV.

insufficient information to determine why there was liquid water at low levels but none aloft after 1700. After 1900, all liquid water was gone, and the potential for weather modification probably went to zero (or may have become negative).

IV. SUGGESTIONS FOR FUTURE RESEARCH

For some cases in the existing data set, it would be useful to assess how much the precipitation processes could be altered by cloud seeding in the regions of observed supercooled liquid water. This might be evaluated by using an airflow model with a microphysical particle growth model for various seeding dosages and locations. The result would be some suggestions for an optimal seeding strategy.

The entire existing data set could be reviewed from a 'climatological' perspective to evaluate the relative precipitation efficiency of natural storms and the likelihood and potential of weather modification opportunities. It would be better if the data set included fall, winter and spring. This kind of information is required for assessing the practicability of operational cloud seeding and a cost/benefit analysis.

Data sets could be combined for computer analysis with fine time/space resolution to study small scale precipitation physics (e.g., radar, satellite and radiometer data). It is vital to know what the relationship is between regions of existing precipitation and regions of supercooled liquid water. It is also important to know how representative a small sample is of a larger scale cloud system. This effort would involve some reprocessing of raw Ka-band radar data. Some new techniques will have to be designed for combining data from different sources and accounting for differences in resolution, sampling rate and geometry. As a first step, this analysis could be tried on one of the smaller and perhaps simpler cases from 1985.

It would be worthwhile to evaluate the use of satellite data to

infer some microphysical cloud characteristics (for example, ice nucleation and supercooled liquid water from cloud top temperature). Satellite data have not yet been thoroughly exploited. Existing data sets could be used for 'ground truth' in comparing with enhancements of archived satellite data. The results would help other analysis and would provide operational guidance in forecasting favorable events.

It is suggested that a common time reference should be adopted for all field data, either GMT or MST. Having both times present in the data set imposes awkwardness and likelihood of error to the data analysis.

In the routine data analysis, there are advantages in using the smallest time resolution possible. Then the chance to study fine scale structures is not precluded by averaging or skipping records. Imagine the hypothetical case of an extensive cloud characterized by a checkerboard pattern where concentration maxima of liquid water alternate with concentration maxima of precipitation size ice. (This is not a far fetched case.) If the sampling intervals of the radiometer and radar are too long duration or out of phase, then the data could suggest several different and equally misleading scenarios: (1) a homogeneous cloud with a balance of ice and water, (2) a cloud of convective scale elements which contain both ice and water, (3) a mixed cloud with varying proportions of ice and water which change with time.

REFERENCES

Cooper, W.A. and C.P.R. Saunders, 1980: Winter storms over the San Juan Mountains. Part II: Microphysical processes. J. Appl. Meteor., 19, 927-941.

D'Errico, R.E., 1978: An observational study of the accretional properties of ice crystals of simple geometric shapes. Preprints, Conf. on Cloud Physics and Atmos. Electricity, Issaquah, Washington, Amer. Meteor. Soc., Boston, 114-121.

Fukuta, N. and R. Winther, 1985: Ground Microphysical Observation in 1985 Utah/NOAA Cooperative Weather Modification Research Program, Final Report, Department of Meteorology, University of Utah, Salt Lake City, Utah, 44pp.

Grant, L.O. and P.W. Mielke, Jr., 1982: A Program for Federal State Local Cooperative Weather Modification Research. Department of Atmospheric Science, Colorado State University, Fort Collins, Colorado 70pp.

Hill, G.E., 1982: Evaluation of the Utah operational weather modification program. Final Report. Utah Water Research Laboratory, Utah State University, Logan, Utah 291pp.

Long, A., 1984: Physical investigations of winter orographic clouds in Utah. Final Report. Atmospheric Sciences Center, Desert Research Institute, Reno, Nevada 286pp.

Magono, C. and C.W. Lee, 1966: Meteorological classification of natural snow crystals. J. Fac. Sci., Hokkaido Univ., Series VII, 2, 321-362.

Rauber, R.M. and L.O. Grant, 1983: Preliminary analysis of the hypothesis used in the Utah operational weather modification program. Department of Atmospheric Science, Colorado State University, Fort Collins, Colorado, 123 pp.

Rauber, R.M. and L.O. Grant, 1985: Precipitation augmentation potential of wintertime storms over the Tushar Mountains of Utah. Department of Atmospheric Science, Colorado State University, Fort Collins, Colorado, 167pp.

Sassen, K., 1986: Lidar and Supporting Observations of Winter Storms from the 1985 Utah/NOAA Cooperative Weather Modification Program. Final Report, Department of Meteorology, University of Utah, Salt Lake City, Utah, 73pp.

Solak, M.E. and R.B. Allan, 1985: The Detection of Supercooled Liquid Water, Ground Based Ice Accretion Measurements in the Tushar Mountains near Beaver, Utah and Calculations of Supercooled Liquid

Water Concentrations in Winter Orographic Clouds during the period 15 January - 15 March 1985. Atmospherics Incorporated, Fresno, California 46pp.

Swart, H.R., 1985: Utah/NOAA Field Research Operations Report, 1985. North American Weather Consultants, Salt Lake City, Utah.